

# HEMATITE THROUGH THE EYES OF THE EXOMARS 2020 ROVER ROSALIND FRANKLIN: Simulating mineral identification with the PanCam WAC multispectral filters



Roger Stabbins<sup>1</sup>, Sara Motaghian<sup>1</sup>, Peter Grindrod<sup>1</sup>, and the PanCam Science Team

<sup>1</sup>Department of Earth Sciences, Natural History Museum, London, UK

(r.stabbins@nhm.ac.uk)

## 1. INTRODUCTION

We present a pipeline for investigating the ability of PanCam to discriminate one particular mineral species against a defined set of background materials. We demonstrate the pipeline for the mineral hematite, an iron oxide indicative of changes in oxidation conditions, with implications for past habitability, and a target of interest for the *Curiosity* rover at Vera Rubin Ridge<sup>1,2</sup>.

## 2. PANCAM

*PanCam*<sup>3</sup> is the mast-mounted colour-stereo panoramic camera system for the ExoMars 2020 Rosalind Franklin rover<sup>4</sup>, with an objective of visual geological characterisation, focusing on signatures of ancient habitats. PanCam will measure the VNIR (380nm - 1100nm) spectral reflectance of surfaces with a multispectral suite of 12 narrowband filters<sup>5</sup>.

## 3. SPECTRAL PARAMETERS

Spectral parameters (SPs) are operations that measure certain features of a mineral reflectance spectrum. Thus, well chosen SPs provide a low-dimensional method of comparing and distinguishing minerals. A set of recommended SPs for the mineralogy of Mars have been reported for application to *CRISM* hyperspectral orbital data<sup>6-7</sup>, a number of which span the VNIR, illustrated in Figure 1. Figure 2 illustrates how an SP operation applied across a hyperspectral image can discriminate minerals.

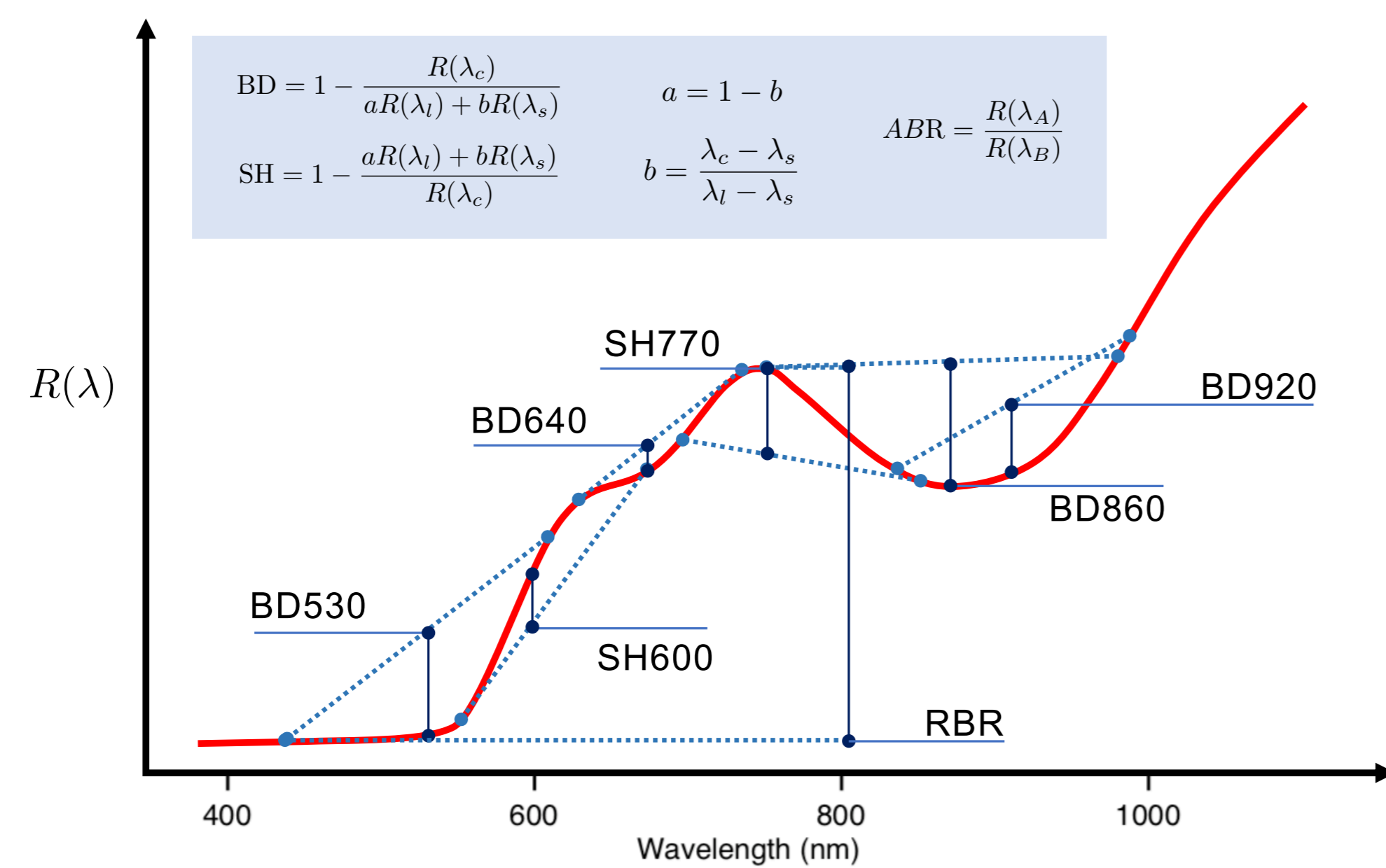


Figure 1. Illustration of the *CRISM* VNIR spectral parameters on an exemplary hematite spectra (RPN\_OOX\_04). BD= Band Depth, SH= Shoulder Height, R= Ratio. See 6-7.

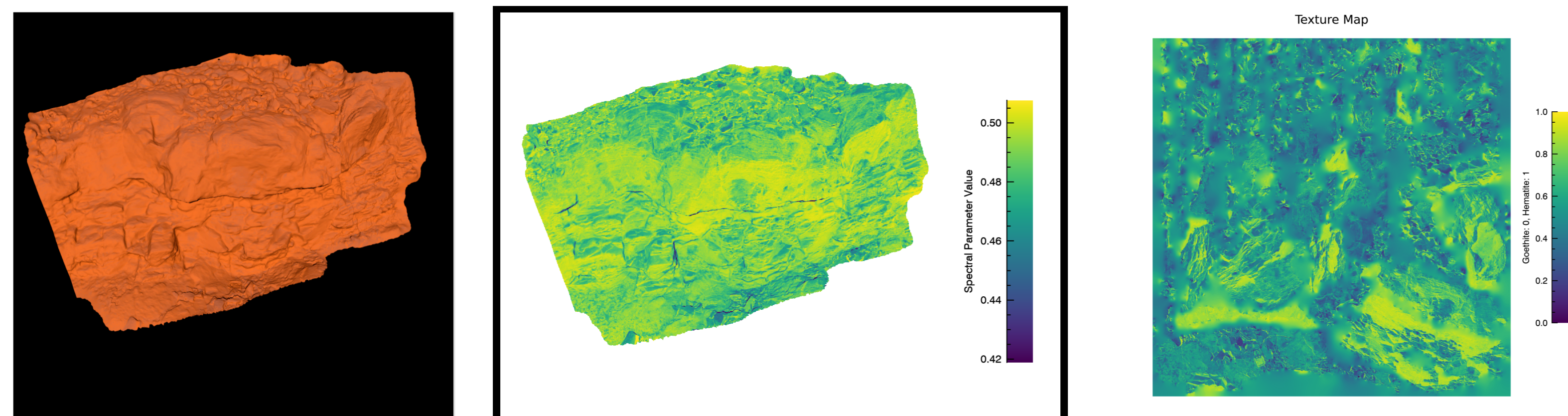


Figure 2. Simulated rock outcrop hosting a mixture of hematite and goethite. Left shows *sRGB* colour image under uniform illuminant, demonstrating the inability of the colour space to discriminate between the materials. Centre gives the *SH600* spectral parameter map of the outcrop, mapped to a viridis colour scale. Right gives the ground-truth texture of mineral mixing. Simulation rendered in an adapted distribution of spectral-PBRT at hyperspectral resolution<sup>8</sup>.

## 4. PROBLEM STATEMENT

The *CRISM* SP set was curated for hyperspectral data, but *PanCam* is multispectral, sampling the morphology at much lower resolution. Here we investigate the robustness of the SPs of Figure 1 at discriminating hematite against a set of expected minerals of the ExoMars landing site at *Oxia Planum*<sup>9-10</sup>. Laboratory mineral spectra are drawn from a database (see Figure 3) and sampled with Gaussian filters according to the *CRISM* recommended wavelengths and FWHM, and the nearest corresponding filters of *PanCam*, as shown in Table 1. Information for the *Curiosity* rover *Mastcam* multispectral filters are included for comparison.

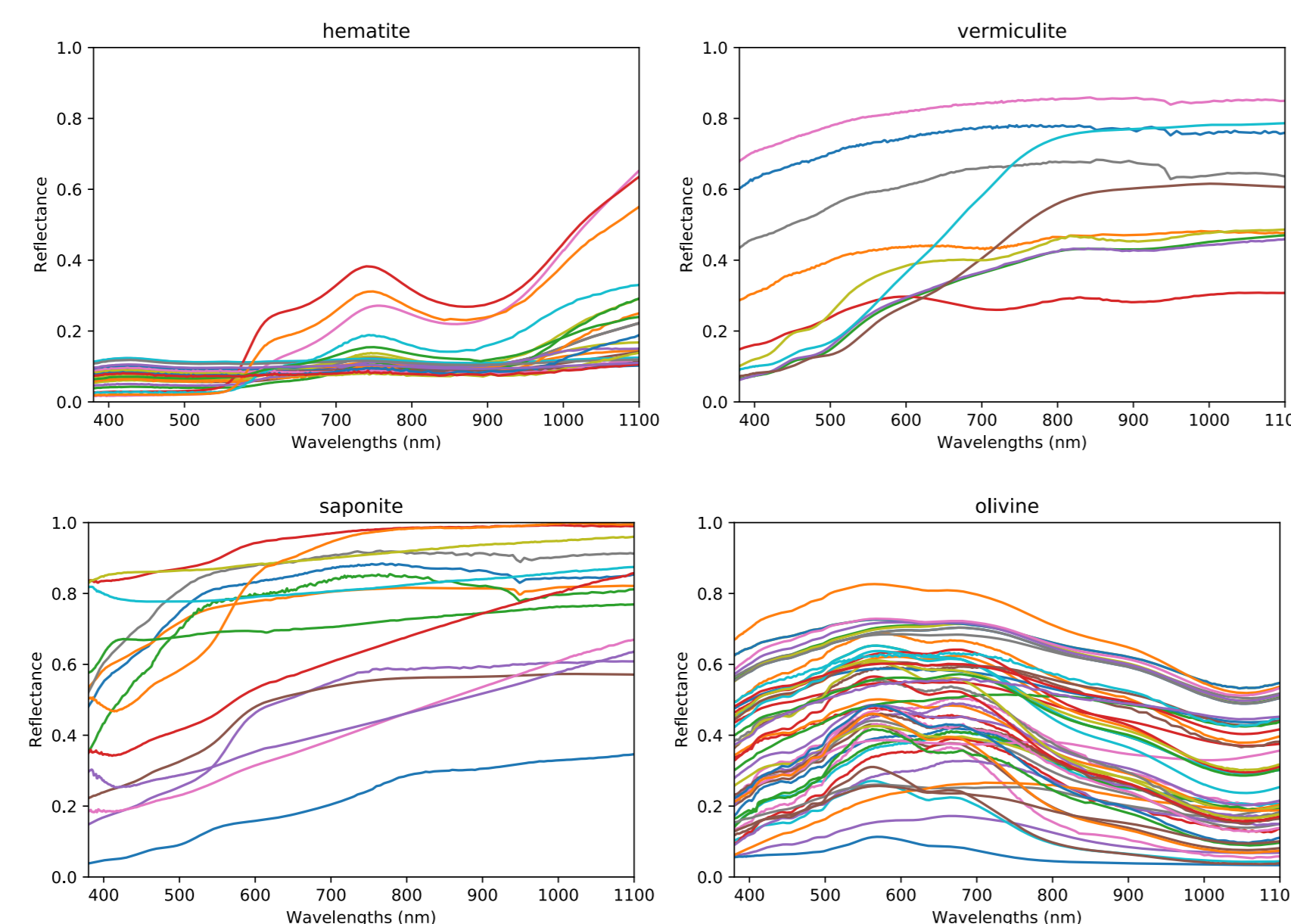
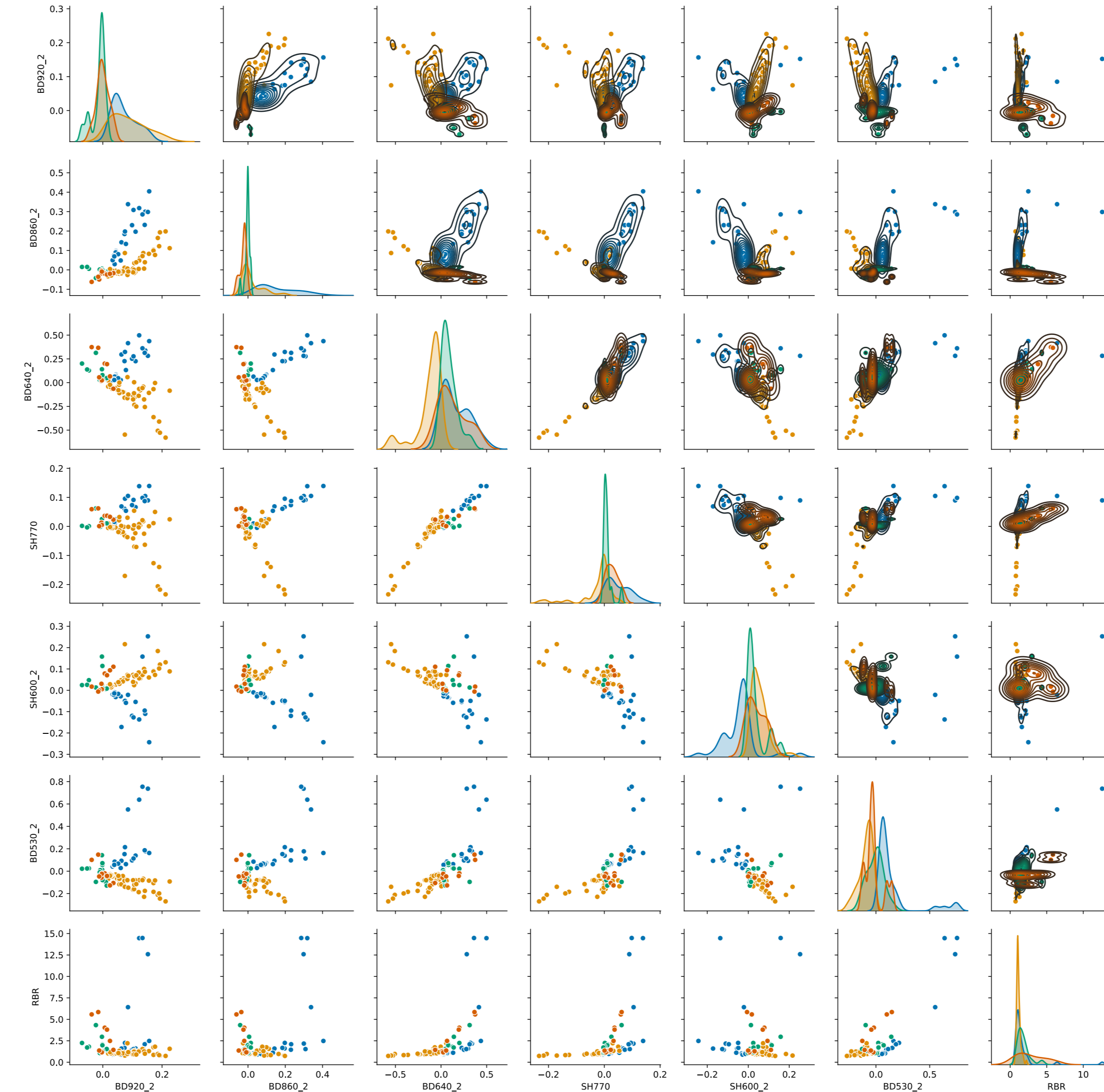


Figure 3. Input mineral reflectance data for target (hematite) and background (vermiculite, saponite and olivine). Data sourced via the *Western Washington Spectral Database*<sup>11</sup>, a compilation of several widely used spectral libraries, including USGS *speclib06*<sup>12</sup>, and *HOSERlab*<sup>13</sup>.

## CRISM (HYPERSPECTRAL)



## PANCAM (MULTISPECTRAL)

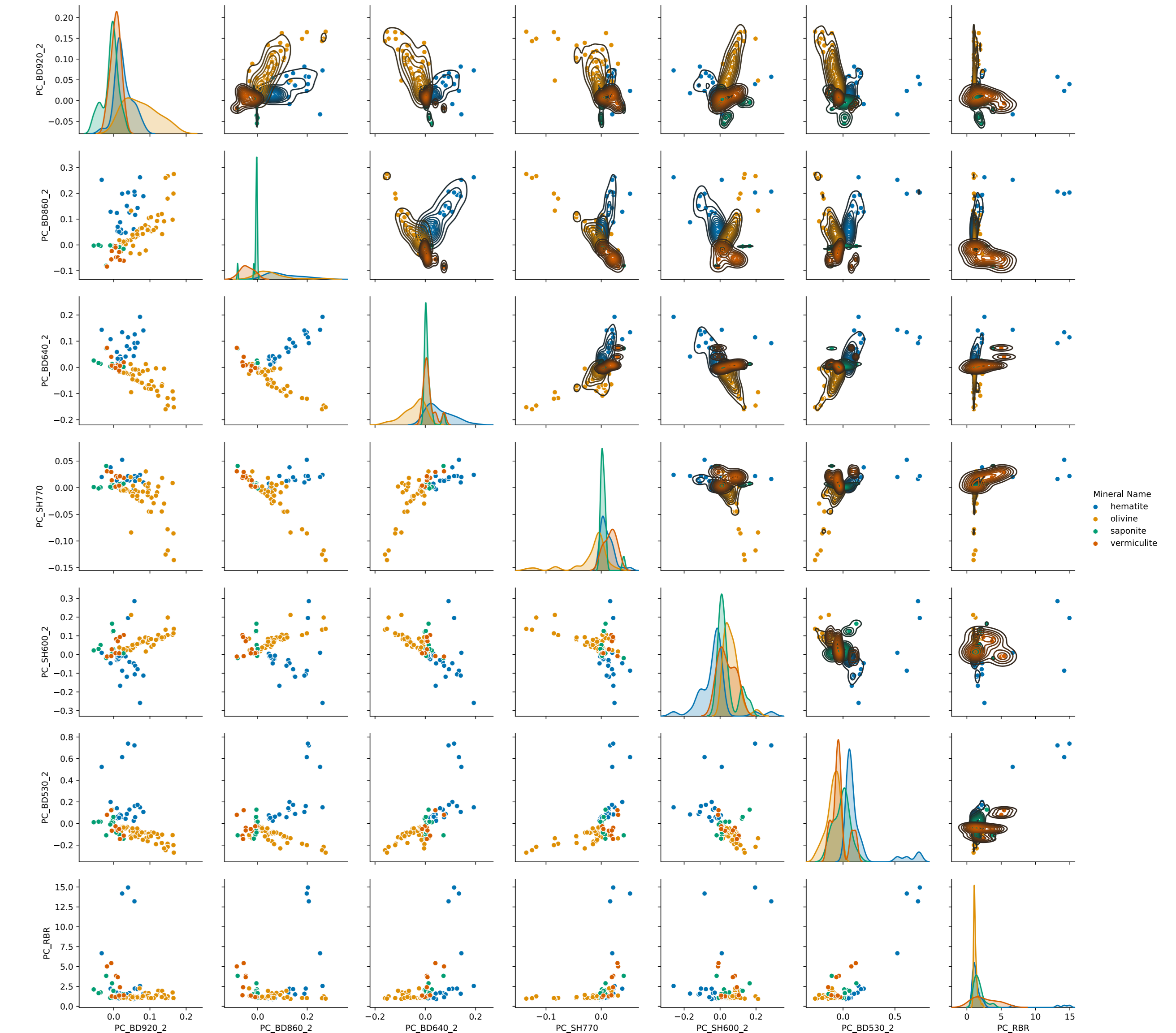


Figure 4. Paired scatterplots of the SPs computed with *CRISM* and *PanCam* sampling, indicating data distribution of hematite (blue) against background minerals (orange, green, red) across the SP vector space. Univariate plots (diagonal) indicate single SP discrimination, bivariate indicate advantage of combining SPs. Upper gives density contours.

## 5. VISUALISATION

A Python software pipeline is in development, utilizing the *Pandas* library for multivariate data analysis. Figure 4 gives a visual comparison of the computed SPs for *CRISM* and *PanCam* sampling, demonstrating the ability of each system to discriminate hematite against the background minerals, via clustering in the SP vector space. Single SPs (diagonal) indicate poor discrimination. Combined SPs, such as *BD530/BD860*, indicate robust discrimination. Figure 5 visualizes the consistency of SP measurements between *CRISM*, *PanCam* and *Mastcam*, indicated by deviation from linearity.

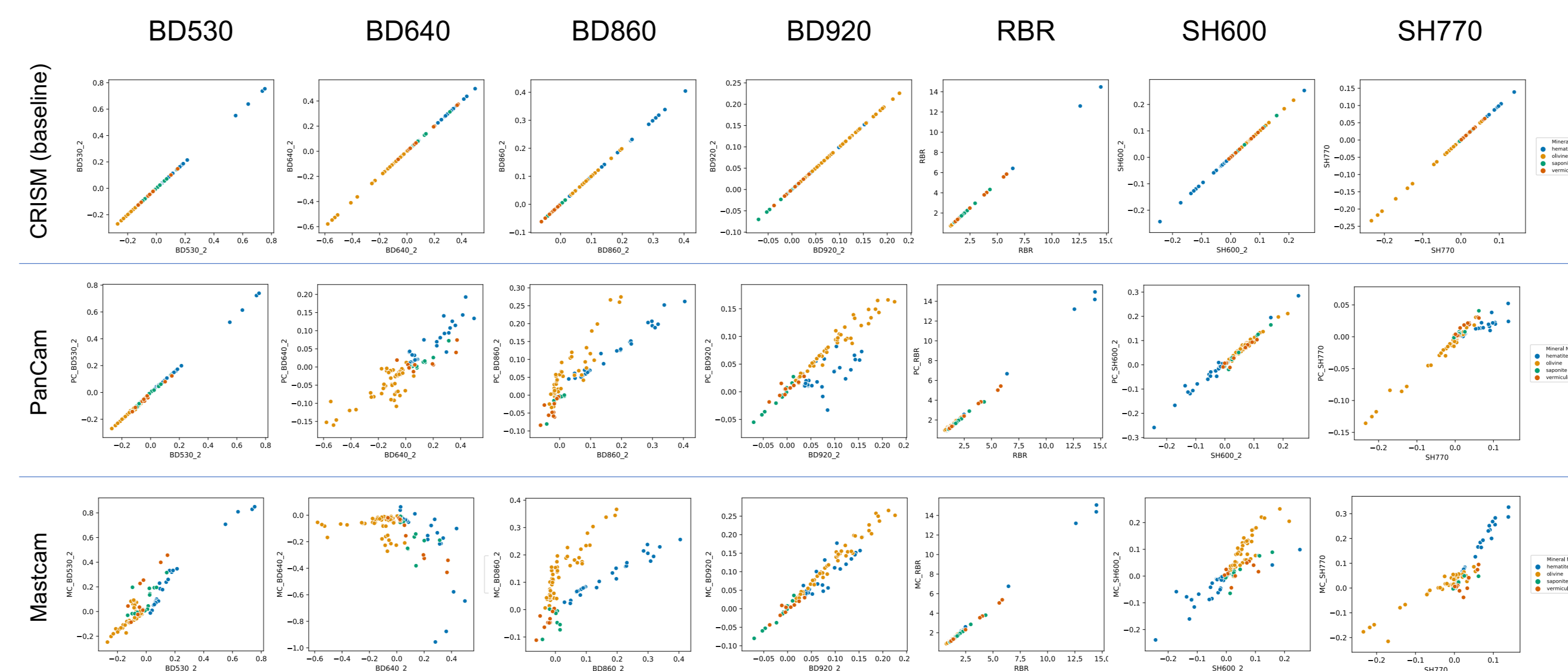


Figure 5. Plotting SPs of each instrument against the *CRISM* SPs provides a visualization of the consistency of SP evaluation between instruments. *CRISM* vs *CRISM* explicitly shows the expected linear relationship, with axes indicating the expected range. Notably, *Mastcam* poorly captures *BD640*, and both instruments poorly capture *BD860*. Despite this, Figure 4 demonstrated the utility of *BD860* in hematite discrimination, which is ultimately the more important metric of success.

Table 1. SP wavelengths for *CRISM* data, and nearest matches for *PanCam* and *Mastcam*.

| CRISM Spectral Parameters | Nearest Mastcam Filters |     |      |    | Nearest PanCam Filters |      |     |      |      |
|---------------------------|-------------------------|-----|------|----|------------------------|------|-----|------|------|
|                           | Spectral Parameter      | CWL | FWHM | ID | CWL                    | FWHM | ID  | CWL  | FWHM |
| BD530_2                   | $\lambda_B$             | 440 | 5    | L2 | 445                    | 20   | L04 | 500  | 20   |
|                           | $\lambda_C$             | 530 | 5    | L1 | 527                    | 14   | L01 | 570  | 12   |
|                           | $\lambda_I$             | 614 | 5    | L4 | 676                    | 20   | L03 | 610  | 10   |
| RBR                       | $\lambda_B$             | 440 | 5    | L2 | 445                    | 20   | L06 | 440  | 25   |
|                           | $\lambda_A$             | 770 | 5    | L3 | 751                    | 20   | R02 | 740  | 15   |
| SH600_2                   | $\lambda_B$             | 530 | 5    | L1 | 527                    | 14   | L02 | 530  | 15   |
|                           | $\lambda_C$             | 600 | 5    | L4 | 676                    | 20   | L03 | 610  | 10   |
|                           | $\lambda_I$             | 716 | 3    | L3 | 751                    | 20   | R02 | 740  | 15   |
| SH770                     | $\lambda_B$             | 716 | 3    | L4 | 676                    | 20   | R03 | 740  | 15   |
|                           | $\lambda_C$             | 775 | 5    | L3 | 751                    | 20   | R02 | 780  | 20   |
|                           | $\lambda_I$             | 860 | 5    | L5 | 867                    | 20   | R01 | 840  | 25   |
| BD640_2                   | $\lambda_B$             | 600 | 5    | L1 | 527                    | 14   | L03 | 610  | 10   |
|                           | $\lambda_C$             | 624 | 3    | L4 | 676                    | 20   | L05 | 670  | 12   |
|                           | $\lambda_I$             | 780 | 5    | L3 | 751                    | 20   | R03 | 740  | 15   |
| BD860_2                   | $\lambda_B$             | 755 | 5    | L3 | 751                    | 20   | R02 | 740  | 15   |
|                           | $\lambda_C$             | 860 | 5    | L5 | 867                    | 20   | R01 | 840  | 25   |
|                           | $\lambda_I$             | 977 | 5    | R5 | 937                    | 22   | R05 | 940  | 50   |
| BD920_2                   | $\lambda_B$             | 807 | 5    | R3 | 805                    | 20   | R01 | 840  | 25   |
|                           | $\lambda_C$             | 920 | 5    | R5 | 937                    | 22   | R05 | 940  | 50   |
|                           | $\lambda_I$             | 984 | 5    | R6 | 1013                   | 42   | R06 | 1000 | 50   |

## 6. CONCLUSIONS & FUTURE WORK

The method presented in this work, for the specific case of hematite in contrast to minerals expected at *Oxia Planum*, is extendable to arbitrary targets and background sets: software is in development for scaling the method to large sets (i.e. more comprehensive background mineralogy), and for exploring the wider SP phase-space by varying the filters. Quantitative measures of clustering will enable scoring of SPs and combinations, enabling a recommendation of *PanCam* filters required to discriminate a target against an expected background.

**Acknowledgement:** This work is funded by a UK Space Agency *Aurora* Grant.

## REFERENCES

- Fraeman et al, 2013, *Geol.*, 2. Fraeman et al, 2018, *LPSC49*, 1557, 3. Coates et al, 2017, *Astrobiology*, 4. Vago et al, 2017, *Astrobiology*, 5. Cousins et al, 2012, *Plan. & Space. Sci.*, 6. Pelky et al, 2007, *JGR-Planets*, 7. Vivano-Beck et al, 2014, *JGR-Planets*, 8. Stabbins et al, 2018, *LPSC49*, 2099, 9. Quantin- Nataf et al, 2019, *Mars-9*, 6317, 10. Mandon et al, 2019, *Mars-9*, 6173, 11. Rice et al, 2016, <http://spectro.geol.wvu.edu/>, 12. Clark et al, 2007, USGS Digital Spectral Library, 13. Cloutis et al, 2006, *LPSC37*, 2121